15th International Plansee Seminar, Eds. G. Kneringer, P. Rödhammer and H. Wildner, Plansee Holding AG, Reutte (2001), Vol. 1

Production of Diamond Wire by Cu15 v-% Nb "In situ" Process

Marcello Filgueira*, Daltro Garcia Pinatti+

*Universidade Estadual do Norte Fluminense, CCT-LAMAV, RJ, Brazil

+FAENQUIL, Departamento de Engenharia de Materiais, SP, Brazil

Summary:

Diamond wires are cutting tools used in the slabbing of dimension stones, such as marbles and granites, as well as in cutting of concrete structures. This tool consists of a steel cable on which diamond annular segments (pearls) are mounted with spacing between them. This work has developed a new technological route to obtain the diamond wires, whose fabrication involves metal forming processes such as rotary forging and wire drawing, copper tubes restacking, and thermal treatments of sintering and recrystallization. It was idealized the use of Cu 15v% Nb composite wires as the high tensile strength cable, covered with an external cutting rope made of bronze 4wt% diamond composite, along the overall wire surface. Investigations were carried out on the mechanical behavior and on the microstructural evolution of the Cu 15 vol % Nb wires, which showed ultimate tensile strength (UTS) of 960 MPa and deformation of approximately 3,0 %. The cutting external rope of 1.84 mm in diameter showed UTS = 230 MPa. On the microstructural side aspect it was observed that the diamond crystals were uniformly distributed throughout the tool bulk in the several processing steps. Cutting tests were carried out starting with an external diamond rope of 1.93 mm in diameter, which cut a marble sectional area of 1188 cm^2, and the tool degraded to a final diameter of 1.23 mm. For marble the "in situ" wire showed a probable performance 4 times higher than the diamond saws, however their probable performance was about 5 to 8 times less than the conventional diamond wires due to the low abrasion resistance of the bronze matrix and the low adhesion between the pair bronze-diamond.

Keywords:

Diamond wire, Cu-Nb composite, bronze-diamond composite, wire drawing, restacking, sintering

15th International Plansee Seminar, Eds. G. Kneringer, P. Rödhammer and H. Wildner, Plansee Holding AG, Reutte (2001), Vol. 1

1. Introduction:

Diamond wires are cutting tools for rocks (marble, granite etc.), concrete and substitutes of saws in general (1-5). They are composed of an AISI 316 stainless steel cable over which are assembled diamond sintered pearls with 10 to 12 mm in diameter spaced 25 mm between each one. In this work we present an alternative route to manufacture diamond wire called "in situ technique" derived from the fabrication of superconductor wire by the powder metallurgy process. The core wires are manufactured with Cu15v-%Nb powder and the external capping wire is made of bronze 4wt% diamond. The wires are fabricated by drawing with minor steps of swaging after each assembly during the composite fabrication. Table 1 gives the comparison of geometric data of diamond wires fabricated by pearls and "in situ" techniques. Diamond volume and surface in the "in situ" wire are 20 to 30 times larger than pearls wire, and cutting section of rocks are decreased by 40%.

Table 1 Comparative geometric data between pearls- and "in situ"- diamond wire

Data	Pearls	"In situ"	
ϕ_e (external diameter)	10 mm	8 mm	6 mm
ϕ_i (internal diameter)	7 mm	5 mm	3 mm
Width	5 mm(pearls)	1000 mm (length/m)	
Spacing	25 mm	Continuous	
Diamond volume/m *	1000 mm^3	30,630 mm^3	21,206 mm^3
Diamond surface/m +	785 mm^3	25,133 mm^3	18,850 mm^3
Relation between "in situ"/pearls	Volume	30	21
	Surface	32	24

*Diamond volume/m: $\pi/4 \times (\phi_e^2 - \phi_i^2) \times$ width x nr. pearls/m
+Diamond surface/m: $\pi \times \phi_e \times$ width x nr. pearls/m

2. Materials and Methods:

Cu15v-%Nb core wires Niobium and copper compositions are given in Table 2. They meet the specification of high purity Nb and OFHC Cu in order to achieve high rate of area reduction (initial cross section/final cross section $R = 5 \times 10^8$). Grain size distribution of bronze powder has 80% of the particles in the 75/60 μm range. Fig.1 presents the processing route of the Cu-Nb composite. Area reduction between each pass was S = 10%. Intermediate

15th International Plansee Seminar, Eds. G. Kneringer, P. Rödhammer and H. Wildner, Plansee Holding AG, Reutte (2001), Vol. 1

and final copper proportion was determined by etching with $1H_2O + 1HNO_3$ solution (6,7).

Table 2 Chemical composition of niobium and copper (wt%)

	Ta	Fe	W	Mo	Ag	Al	Zr	Ti	C	N	O	Sn
Niobium	0.11	0.005	0.02	0.009	nd	-	-	0.004	0.02	0.01	0.012	nd
Copper	nd	0.002	nd	nd	0.003	nd	nd	-	0.002	-	0.002	nd
Bronze	-	0.008	-	-	-	-	-	-	0.03	0.01	0.04	10.8

nd not detected; -absent; C (LECO CS-244); N, O (TC-136); other elements inductively coupled plasma optical emission spectrometry (ICP/OES)

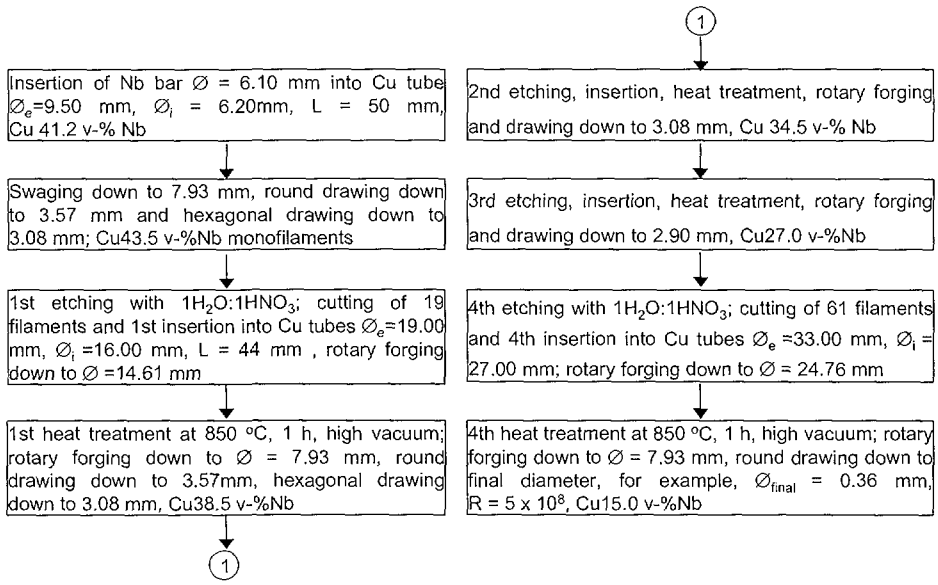

Fig. 1 Processing route of Cu-Nb composite by "in situ" technique

Diamond external bronze capping Table 3 gives the typical concentration versus density of diamond in cutting tools. In the present work we used a concentration of 50 (2.2 carat/cm^3; 0.44 g/cm^3; 0.1264 cm^3 of diamond/cm^3 of tools) since this is the concentration used for granite rocks. For marble it is used a concentration of 30. Figure 2 shows the processing flow chart of the bronze/diamond cap starting with bronze 4 wt% diamond. Table 4 gives an example of calculation of the mass of diamond and its percentage with respect to the bronze.

15th International Plansee Seminar, Eds. G. Kneringer, P. Rödhammer and H. Wildner, Plansee Holding AG, Reutte (2001), Vol. 1

Table 3 Typical concentration versus density of diamonds in cutting tools

Concentration of diamond	Mass of diamond/cm^3 of tool volume		Volume of diamond (cm^3)/tools (cm^3)
	Carat	Grams	
150	6.6	1.32	0.38
125	5.5	1.10	0.32
100*	4.4	0.88	0.25
75	3.3	0.66	0.19
50	2.2	0.44	0.13
42	1.85	0.37	0.11
30	1.32	0.26	0.07
25	1.10	0.22	0.06

*Concentration of 100 refers to 25 % in volume of diamond per cm^3 of tool and has 4.4 carat of diamond / cm^3 of tools; 1 carat = 0.2 g. The fourth column is obtained dividing the third column by the diamond density ($\rho_{diam.}$ = 3.48 g/cm^3)

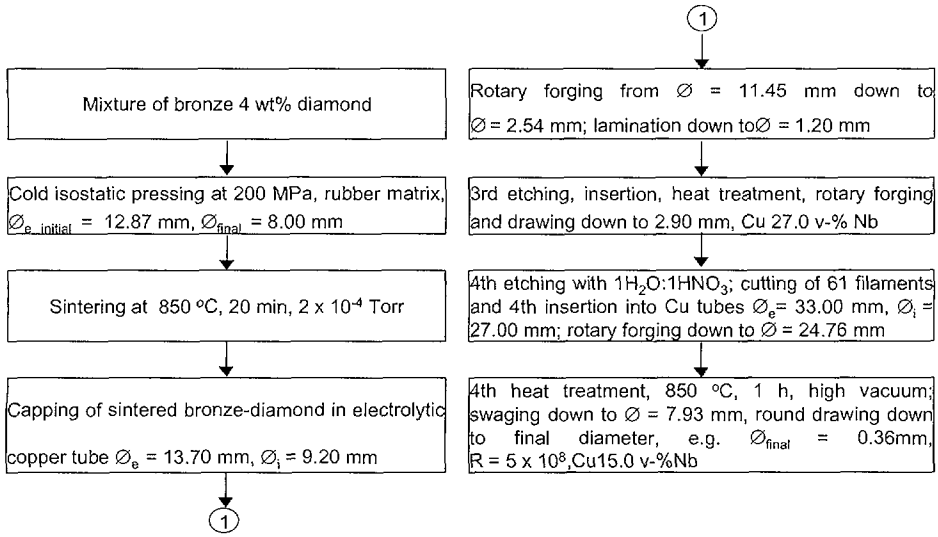

Fig. 2 Processing flow chart of the bronze / diamond external cap

15th International Plansee Seminar, Eds. G. Kneringer, P. Rödhammer and H. Wildner, Plansee Holding AG, Reutte (2001), Vol. 1

Table 4 Calculation of bronze-diamond composition

Volume of the bronze bar before compactation

$$V_{BR} = \frac{\pi\varphi^2}{4}.\ell = \frac{\pi(1.287)^2}{4}.20 = 26\ cm^3$$

Bronze mass (neglecting the diamond mass for a first approximation)

$$m_{BR} = V_{BR} \times \rho_{ap.BR} = 26\ cm^3 \times 2.55\ g/cm^3 = 66.3\ g$$

Volume of compacted bronze

$$V_{comp.BR} = \frac{m_{BR}}{\rho_{comp.BR}} = \frac{66.3\ g}{8.80\ g/cm^3} = 7.53\ cm^3$$

$$V_{diam.} = V_{comp.BR} \times \rho^{vol.}_{diam.} = 7.53\ cm^3 \times 0.1264\ cm^3\ of\ tool = 0.9518\ cm^3$$

$$m_{diam,} = V_{diam.}\ \rho_{diam.} = 0.9518\ cm^3 \times 3.48\ g/cm^3 = 3.31\ g$$

Percentage of diamond in the bronze - $\frac{3.31}{66.30+3.31} = 0.0475 = 4.75$ wt%

Obs.: Correction of mass bronze with the diamond mass results in a final value of 4.76 wt%

Geometric array of Cu15v-%Nb and bronze/diamond braided wire Two arrays are possible. Fig. 3a shows a monolithic array with 61 filaments of Cu15v-%Nb (ϕ =1.55 mm, hexagonal shape), corresponding to a diameter of 13.95 mm. These 61 filaments of Cu15v-%Nb are involved by 12 wires of bronze 4 wt% diamond (4.90 mm in diameter) in the sintering step and heat treated at 850°C for 20 min condition. The set is inserted in a copper tube ($\phi_{ext.}$ = 30 mm and $\phi_{int.}$ = 25 mm) as shown in Fig. 3b. The monolithic array is swaged till 30% in area reduction and sintered at 850°C for 1 hour in vacuum of 10^{-4} Torr to assure the cohesion of the filaments. In the sequence the set is drawn and heat treated at 650°C for 20 min achieving an area reduction of 30%. The final drawing diameter is ϕ = 6.90 mm; after pickling with $1H_2O$ + $1HNO_3$ the diameter is reduced to 6.00 mm. The braided array shown in Fig. 4 is composed of 127 filaments of Cu15v-%Nb (ϕ = 0.36 mm each filament forming a core of 4.68 mm in diameter. In the sequence 12 wires of bronze 4 wt% diamond (ϕ = 1.65 mm each filament) are braided around the core giving a final diameter of 8.00 mm. Braided wires are the substitute of conventional diamond wire since it is more flexile than the monolithic array. Steel wires have a resistance of 1800 to 2000 MPa but they are not used in conventional diamond wire due to oxidation and low flexibility. Normally stainless steel is used. The Cu15v-%Nb combines a resistance close to the steel wire and the flexibility of stainless steel.

15th International Plansee Seminar, Eds. G. Kneringer, P. Rödhammer and H. Wildner, Plansee Holding AG, Reutte (2001), Vol. 1

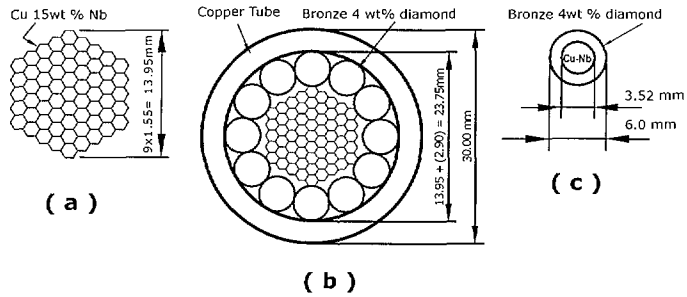

Fig. 3 Sequential array of monolithic "in situ" wire: (a) bee house-type arrangement of Cu15v-%Nb filaments (ϕ=1.55mm) (b) insertion of arrangement (a) and bronze 4 wt% diamond bars into the copper tube (c) final arrangements of monolithic wire (after pickling with $1H_2O + 1HNO_3$)

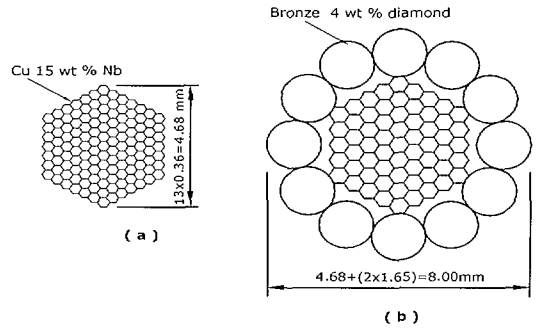

Fig. 4 Sequential array of braided "in situ" wire (a) initial braiding of 127 filaments of Cu15v-%Nb (b) final array of braided wire

3. Results and Discussion:

Cu 15v-% Nb core wire Figs. 5a and b show the microstructure (SEM Zeiss mod. DSM 962) of the cross and longitudinal sections of the Cu15v-%Nb at the area reduction of 1.36×10^6 for a wire diameter of ϕ = 6.08 mm. There are no defects between subassemblies. The dimensions of the Nb ellipsoid ribbons are D = 4.00 μm in width and t = 1.30 μm in thickness (aspect ratio *D/t* = 3). Figs. 5c and d show the same data at an area reduction of 1.27×10^7 for a wire diameter of ϕ = 2.00 mm, D = 2.50 μm, t = 0.80 μm (aspect ratio D/t = 3). This is not sufficient to have the full effect of dislocation in the mechanical resistance of the Cu15v-%Nb (8,9) where D/t=30 with t = 5 to 10 nm. One advantage of this material is that the adjustment of the

15th International Plansee Seminar, Eds. G. Kneringer, P. Rödhammer and H. Wildner, Plansee Holding AG, Reutte (2001), Vol. 1

mechanical properties (ρ, E), R and D/t can be made to better suit the diamond wire. Fig. 6 gives the ultimate tension stress (UTS) as a function of R after the last heat treatment (4th insertion, R = 8.5 x 10^4). The UTS value for pure copper is 500 MPa (R=2250). For Cu10v-%Nb the UTS is 700 MPa (R = 2250) and for Cu15v-%Nb the UTS value is 960 MPa (R = 4800, R_{total} = 8.5 x 10^4 x 4800 = 4.1 x 10^8). The elastic modulus for Cu15v-%Nb is 52.5 GPa. Higher deformation will give higher elastic modulus and less flexibility.

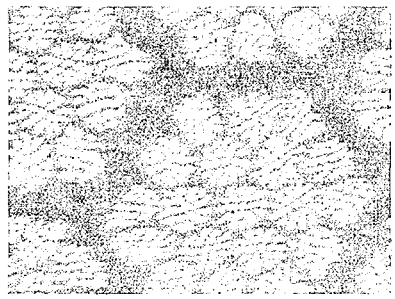

Fig. 5a Cross section of Cu15v-%Nb composite, R=1.36 x 10^6

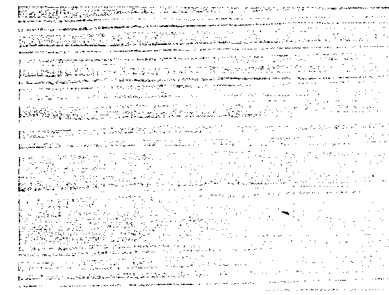

Fig. 5b Longitudinal section of Cu15v-%Nb composite, R=1.36 x 10^6

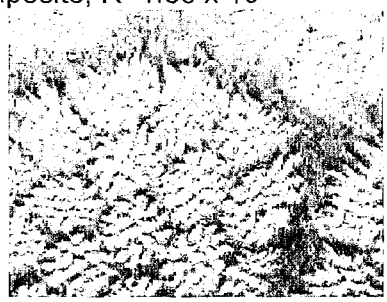

Fig. 5c Cross section of Cu15v-%Nb composite, R=1.27 x 10^7

Fig. 5d Longitudinal section of Cu15v-%Nb composite, R=1.27 x 10^7

15th International Plansee Seminar, Eds. G. Kneringer, P. Rödhammer and H. Wildner, Plansee Holding AG, Reutte (2001), Vol. 1

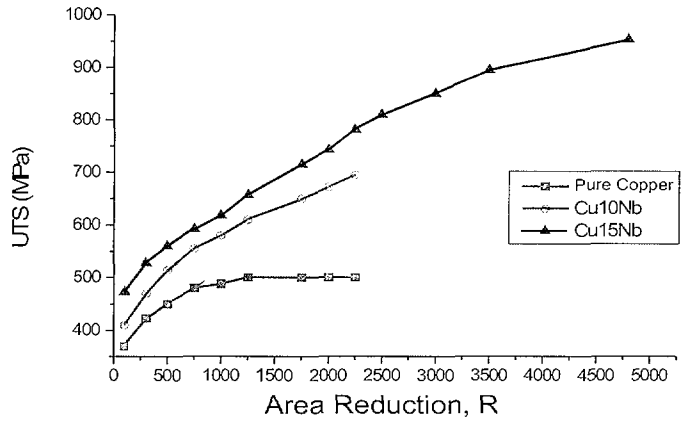

Fig. 6 UTS as a function of area reduction R after the last heat treatment

Bronze 4wt% diamond external cap Fig. 7 shows the longitudinal microstructure of the initial sintered bronze 4 wt% diamond at ϕ = 8.00 mm. The distribution of diamond is relatively spaced. The samples were cupped in Bakelite and ground by 80 mesh emery paper. $1H_2O + 1HNO_3$ pickling did not work because corrosion was not uniform and pitting takes place in the bronze/diamond interface. Fig. 8 shows the cross section of the external cap at ϕ=5.00 mm (R=2.56). Fig. 9 shows the longitudinal section of the external cap and Fig.10 shows the cross section of the diamond wire at ϕ = 1.84 mm (R = 18.90). For bronze 4 wt% diamond the rupture load is shown as a function of the external cap diameter along the various stages of the processing (Fig. 11). The curve of Fig. 11 does not extrapolate to zero but to ϕ = 1.20 mm, whose diameter is the limit of the contact diamond-to-diamond shown in Fig. 13. At this diameter the rupture load is 180 N indicating some adherence between bronze and diamond of the order of 160 MPa ($\sigma \approx 180\ N / [\pi\phi^2 / 4] \approx 180\ N / [(\pi/4)\ (1.20)^2 \times 10^{-6}\ m^2] \approx 160$ MPa). In Fig. 12 the UTS remains constant at 230 MPa up to ϕ = 1.84 mm, after which it decreases. The data of Fig. 12 refers to the UTS values for the same material. This indicates that it is the optimum diameter for this composition and grain size of the diamonds (350 μm).

15th International Plansee Seminar, Eds. G. Kneringer, P. Rödhammer and H. Wildner, Plansee Holding AG, Reutte (2001), Vol. 1

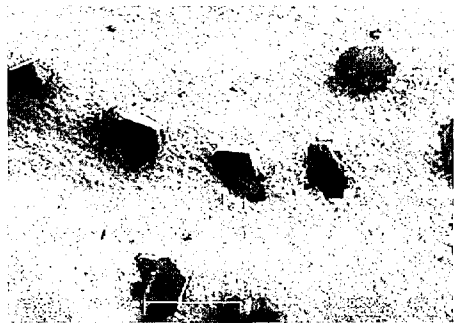

Fig. 7 Longitudinal section of the composite sintered bronze 4 wt% diamond

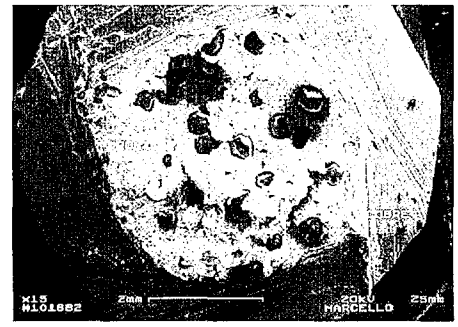

Fig. 8 Cross section of external cap, ϕ = 5.00 mm

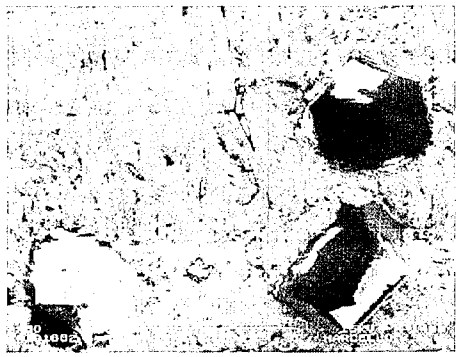

Fig. 9 Longitudinal section of external cap, ϕ = 5.00 mm

Fig. 10 Cross section of diamond composite, ϕ = 1.84 mm

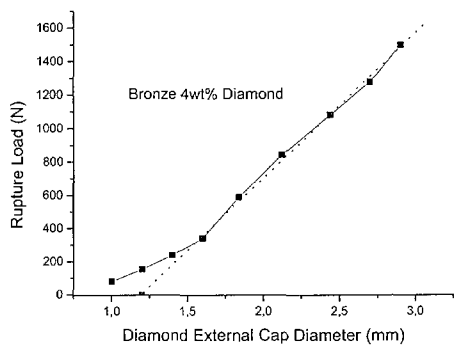

Fig. 11 Rupture load as a function of diamond external cap diameter (mm)

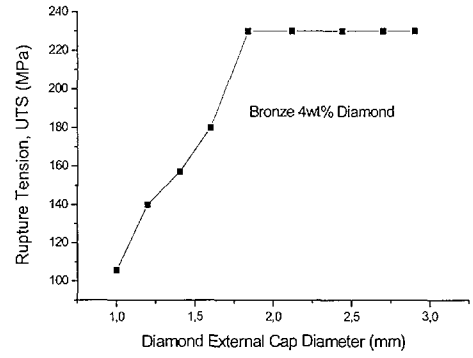

Fig. 12 Rupture tension (UTS) of diamond external cap diameter (mm)

15th International Plansee Seminar, Eds. G. Kneringer, P. Rödhammer and H. Wildner, Plansee Holding AG, Reutte (2001), Vol. 1

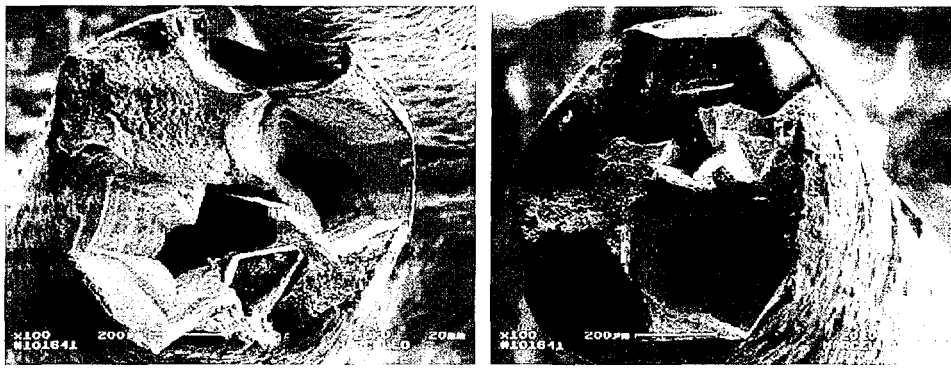

Fig. 13 Examples of fractures of the diamond composite ϕ = 1.20mm

The measurements were made in the annealed condition (650°C for 20 min) and data are an average over 5 to 7 samples. The average modulus of elasticity was E = 11.5 GPa. For annealed commercial bronze UTS=260 MPa and E = 16 GPa (10,11). The presence of diamond up to ϕ 1.84 mm has a minor influence in UTS but it decreases E (more flexible material) since it is now distributed as a composite. Conventional diamond wire has a rupture load between 1200 to 3000 N (UTS=60 to 150 MPa considering ϕ =5.0 mm for the AISI 316 core). The bronze 4 wt% diamond at ϕ = 1.84 mm has a rupture load of 611 N (230 MPa) higher than the AISI 316 core. The UTS = 960 MPa for Cu15v-%Nb core is considerable higher than AISI 316 core.

Bronze - Diamond Adherence Figs.14 through Fig.17 show the interface bronze-diamond in the various stages of the processing (as sintered, ϕ=5mm, ϕ = 3.30 mm and ϕ = 1.84 mm, respectively). The Cu layer is removed with $1H_2O$ + $1HNO_3$ in order to expose the diamond. There is no gap (faults) between bronze and diamond. There is no interdiffusion between them and the adherence is smaller than UTS = 230 MPa of the bronze 4 wt% diamond. In the sequence of development it will be used metal coated diamond or Co-W alloy to improve the adherence.

15th International Plansee Seminar, Eds. G. Kneringer, P. Rödhammer and H. Wildner, Plansee Holding AG, Reutte (2001), Vol. 1

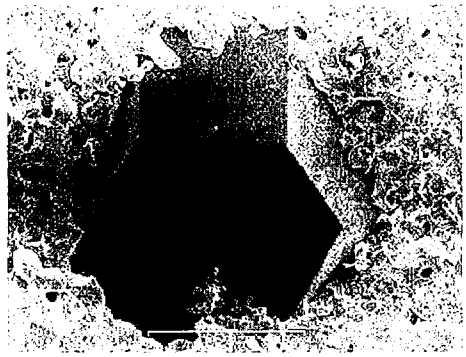

Fig. 14 View of a diamond crystal spiked in the bronze matrix; sample as sintered

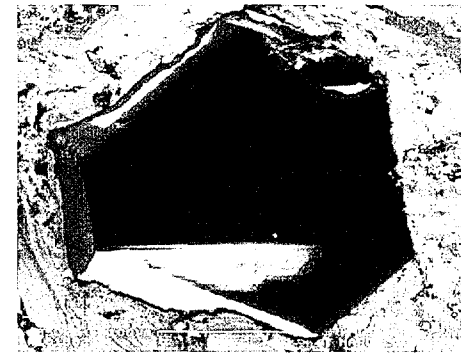

Fig. 15 Bronze – diamond interface ϕ = 5.00mm, longitudinal view

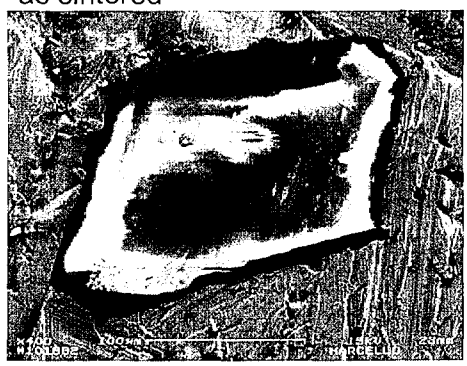

Fig.16 Bronze – diamond interface ϕ = 3.30mm, longitudinal view

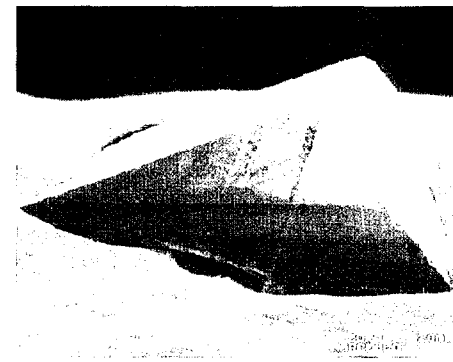

Fig.17 Bronze – diamond interface ϕ = 1.84mm, longitudinal view

Fatigue Strength Figure 18 shows the fatigue tension as a function of the fatigue cycles for bronze 4wt% diamond wire at ϕ = 1.84 mm. Fatigue tests were carried out according to standard ASTM E466-82 (12). Four samples were used for each level of loading: 120-50 MPa, 150-50 MPa, 170-50 MPa, 230-50 MPa, and 60 Hz of frequency. Cycle life close to 10^7 was reached for a tension of 120 MPa. Working tensions were in the range of 24 to 60 MPa indicating that fatigue life is not a limiting factor of the "in situ" bronze 4wt% diamond wire.

15th International Plansee Seminar, Eds. G. Kneringer, P. Rödhammer and H. Wildner, Plansee Holding AG, Reutte (2001), Vol. 1

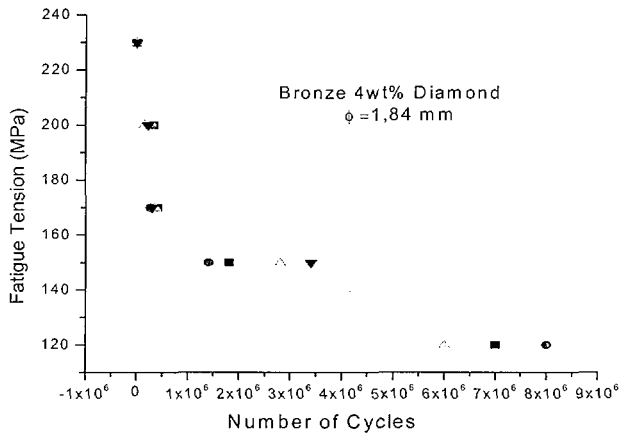

Fig. 18 Fatigue tension as a function of the number of cycles for bronze 4wt% diamond wire, ϕ=1,84mm

Preliminary cutting of marble Table 5 presents the data of marble cutting by a monolithic bronze 4 wt% diamond wire. Figs. 19a, b, c show the micrographs of the wire before, in the middle and in the end of the cutting trial, respectively. This was made in a linear saw frame of 0.22 m in length resulting in 1188 x 10^{-4} m^3/0.22 m = 0.54 m^2/m of cut area per meter of wire. Considering that the braided wires will have 12 bronze 4 wt% diamond wires we expect a cutting area capacity of 6.5 m^2/m. This is 5 (30 m^2/m) to 8 (50 m^2/m) times less than the pearls-diamond wire. The reason for this poor performance is the low abrasion resistance of the bronze material shown in Fig. 19b where abrasion of the loosed diamond powder is clearly seen. Another comparison can be made with results of De Beers (13) for granite cutting with a circular saw of ϕ = 0.7 mm with a diamond volume of v = 1.7 x 10^{-5} m^3 and a perimeter of ℓ = 1.7 mm (v = 10^{-5} m^3/m, effective diamond DAS 100, 40/50 mesh and concentration 30). The measured cutting capacity of the circular saw was 0.62 m^2 resulting in 0.62/1.7 = 0.35 m^2/m. For marble the cutting capacity is doubled (0.73 m^2/m). The cutting capacity of the monolithic "in situ" linear saw frame (0.54 m^2/m for diamond volume of v = 1.7 x 10^{-6} m^3) is 4.4 times higher than the De Beers results [(0.54/1.7 x 10^{-6}) ÷ (0.73/10^{-5})]. In the sequence of development it will be used W, Co, W-Co alloy, Fe, Fe-Co alloy or Nb to improve abrasion. It is recognized that the critical point is the adhesion between the diamond and the matrix. Loosed diamond will catastrophically erode the matrix. Metal coated diamond will improve the cutting area capacity of the "in situ" wire.

15th International Plansee Seminar, Eds. G. Kneringer, P. Rödhammer and H. Wildner, Plansee Holding AG, Reutte (2001), Vol. 1

A new characteristic of the "in situ" diamond wire is its possibility to be welded after rupture. Fig. 19d shows the micrograph of a silver welded part of the "in situ" monolithic wire (ϕ=1.69 mm). Mechanical resistance is maintained (UTS = 226 MPa) in the welded area and diamond of this region is not lost. This characteristic is a considerable improvement over the pearl-diamond wire that is completely lost after rupture.

Table 5 Marble cutting data with the monolithic wire

N	ϕ , mm	σ , mm	$\pm\varepsilon$, mm	A , cm^2
6	1.93	0.06	0.02	0
10	1.79	0.06	0.02	52.5
11	1.78	0.06	0.02	65
20	1.73	0.06	0.01	70.5
22	1.69	0.04	0.01	84
27	1.67	0.05	0.01	104
31	1.67	0.06	0.01	110
31	1.61	0.06	0.01	119
31	1.58	0.06	0.01	118.5
26	1.50	0.08	0.01	126
34	1.44	0.10	0.02	97.5
33	1.38	0.11	0.02	101.25
28	1.31	0.14	0.03	84
18	1.23	0.12	0.03	56.25

N - Number of measurements of ϕ during cutting ε - error: $\frac{\sigma}{(N)^{1/2}}$

ϕ - average diameter $\phi = (\Sigma\phi_i)/N$ σ - variance: $\sigma = \left(\frac{\Sigma[\phi_i - \phi]^2}{N-1}\right)^{1/2}$

15th International Plansee Seminar, Eds. G. Kneringer, P. Rödhammer and H. Wildner, Plansee Holding AG, Reutte (2001), Vol. 1

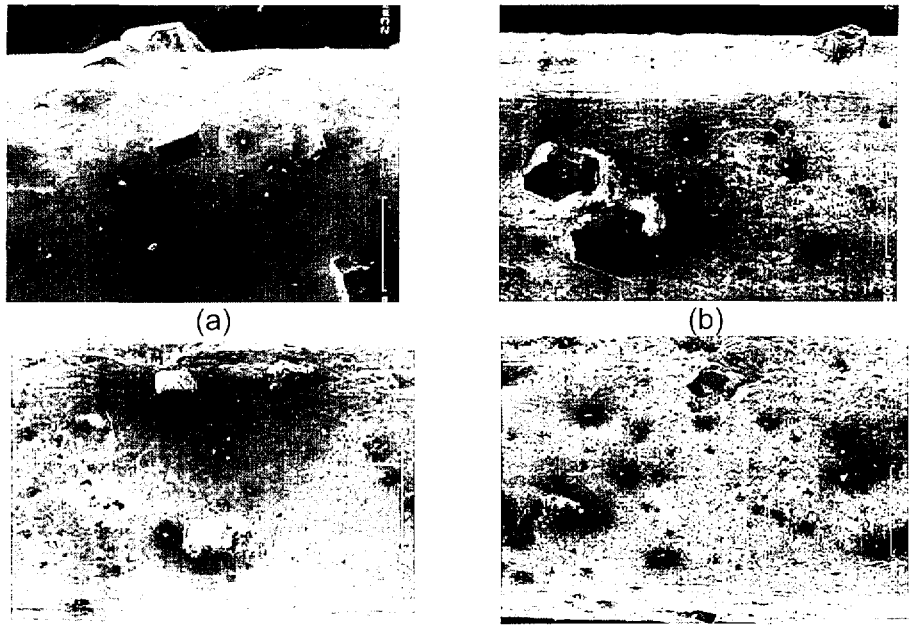

Fig. 19 Marble cutting of monolithic "in situ" wire (a) before cutting operation ϕ = 1.93 mm (b) after cutting an area of A = 605 cm^2, ϕ = 1.61 mm (c) after cutting an area of A=1180 cm^2, ϕ = 1.23 mm (d) silver welded junction of "in situ" monolithic wire

4. Conclusion:

A diamond wire was obtained by an alternative route called "in situ" process by swaging and drawing with maintenance of integrity of the diamond crystal. By this route it is possible to decrease the diameter of the wire from 10 mm to 6 mm decreasing the section of the rock to be cut by 3 times. The core wire made of a Cu15v-%Nb composite allows a compromise between high UTS (960 MPa) and good flexibility (E = 53 GPa). It has the oxidation / corrosion resistance of the AISI 316 and the mechanical resistance of carbon steel. The cap cutting wire was made of bronze 4 wt% diamond and the integrity of the crystal was maintained during swaging and drawing. Abrasion of the bronze matrix was too high indicating the need of development in two directions: use of metal coated diamond in order to improve adhesion and use of another metal matrix such as W-Co, Fe-Co alloys or Nb metal. Cost

15th International Plansee Seminar, Eds. G. Kneringer, P. Rödhammer and H. Wildner, Plansee Holding AG, Reutte (2001), Vol. 1

analysis is under study but it is expected to be lower due to smaller cutting diameter, low cost of drawing process, elimination of pearls and spacing assembly cost, possibility to be welded in case of rupture and final use of the scrap as less noble cutting tools (linear saw frame, etc.).

5. REFERENCES:

1 B. Thoreau: IDR 2 (1984), pp. 94-95
2 P. Daniel: IDR 5 (1986), pp. 187-194
3 P. Daniel: IDR 1 (1986), pp. 1-4
4 P. Daniel: IDR 4 (1993), pp. 200-203
5 M. Pinzari: IDR 5(1989), pp. 231-336
6 S. Pourrahimi et al: Journal of Materials Science Letters 9 (1990) p. 1484
7 M. Filgueira: Ph.D. Thesis (2000), Universidade Estadual do Norte Fluminense, Campos dos Goytacazes, RJ, Brazil, pp. 1-153
8 S. Pourrahimi: Ph.D Thesis (1991), Northeastern University, Boston, MA, pp. 1-175
9 S. Pourrahimi et al: Metallurgical Transactions A 23 (1992), pp. 573-586
10 M.A. Meyers, K.K. Chawla: in "Princípios de Metalurgia Mecânica"(Edgard Blucher Ltda., São Paulo, 1982)
11 W.D. Callister Jr: in "Materials Science and Engineering – An Introduction" (John Willey & Sons, 3rd ed, 1994)
12 ASTM E 466-82. v.03.01: in "Annual Book of ASTM Standards, Section 3 – Metals Test Methods and Analytical Procedures" (1985)
13 Diamond Wear: in Diamond in Industry-Stone (ed. De Beers,1995), pp. 40-43.